Pergamon

Tetrahedron 58 (2002) 4105–4112

TETRAHEDRON

Synthesis and thermodynamic characterization of self-sorting coiled coils

Basar Bilgiçer and Krishna Kumar*

Department of Chemistry, Tufts University, Medford, MA 02155-5813, USA

Received 14 December 2001; accepted 12 January 2002

Abstract—Hydrophobic interactions are a major driving force in protein folding. Amino acid side chains containing trifluoromethyl groups are more hydrophobic than their hydrocarbon counterparts. We describe here the design and characterization of peptide systems with hydrophobic cores composed entirely of leucine or hexafluoroleucine. The preference for homodimeric assemblies over the heterodimer was probed by a disulfide exchange assay. At equilibrium, the homodimers are the dominant species in solution. The fluorinated assembly is much more stable than the hydrogenated peptide dimer and the heterodimer, as judged by thermal and chemical denaturation studies and is responsible for driving the equilibrium in favor of the homodimers. Appropriately fluorinated peptides are therefore useful in stabilizing protein folds and in mediating specific protein–protein interactions.

1. Introduction

Proteins fold to adopt unique three dimensional structures, usually as a result of multiple non-covalent interactions that contribute to their conformational stability.[1] Removal of hydrophobic surface area from aqueous solvent plays a dominant role in stabilizing protein structures.[2,3] For instance, a buried leucine or phenylalanine residue can contribute ~2–5 kcal/mol in stability when compared to alanine. Although hydrogen bonds and salt bridges, when present in hydrophobic environments, can contribute as much as 3 kcal/mol to protein stability, solvent exposed electrostatic interactions contribute far less, usually ≤0.5 kcal/mol.[4,5] Hydrogen bonds between small polar side chains and backbone amides can be worth 1–2 kcal/mol, as seen in the case of N-terminal helical caps.[6] The energetic balance of these intramolecular forces and interactions with the solvent determines the shape and the stability of the fold.

While electrostatic interactions in designed structures can provide conformational specificity at the expense of thermodynamic stability, hydrophobic interactions afford a very powerful driving force for stabilizing structures. Studies originating from our,[7] and other[8] laboratories have recently focused on an unusual source for increasing hydrophobicity, without significant concurrent alteration of protein structure. This is achieved by the introduction of non-proteinogenic, fluorine containing amino acids. The estimated average volumes of CH_2 and CH_3 groups are 27 and 54 Å^3, respectively, as compared to the much larger 38 and 92 Å^3 for CF_2 and CF_3 groups.[9] Given that the hydrophobic effect is roughly proportional to the solvent exposed surface area,[10] the large size and volume of trifluoromethyl groups, in combination with the low polarizability of fluorine atoms, result in enhanced hydrophobicity. Indeed, partition coefficients point to the superior hydrophobicity of CF_3 (Π=1.07) over CH_3 (Π=0.50) groups.[11] The low polarizability of fluorine also results in low cohesive energy densities of liquid fluorocarbons and is manifest in their low propensities for intermolecular interactions.[12,13] These unique properties of fluorine thus simultaneously bestow hydrophobic and lipophobic character to biopolymers with high fluorine content.[14] Previous studies have shown that introduction of amino acids containing terminal trifluoromethyl groups at appropriate positions on protein folds increase the thermal stability and enhance resistance to chemical denaturants.[7,8] Furthermore, specific protein–protein interactions can be programmed by the use of fluorocarbon and hydrocarbon side chains.[15] Because specificity is determined by the thermodynamic stability of all possible protein–protein interactions, a detailed fundamental understanding of the various combinations possible is essential. Here we describe the design, synthesis and thermodynamic characterization of highly fluorinated peptides and their hydrogenated counterparts that have previously been shown to preferentially form homodimers.

2. Results and discussion

2.1. Design principles

The coiled coil motif offers an excellent model system to

Keywords: protein–protein interactions; coiled coils; dynamic self-sorting; de novo protein design.

* Corresponding author. Tel.: +1-617-627-3441; fax: +1-617-627-3443; e-mail: kkumar01@tufts.edu

0040–4020/02/$ - see front matter
PII: S0040-4020(02)00260-0

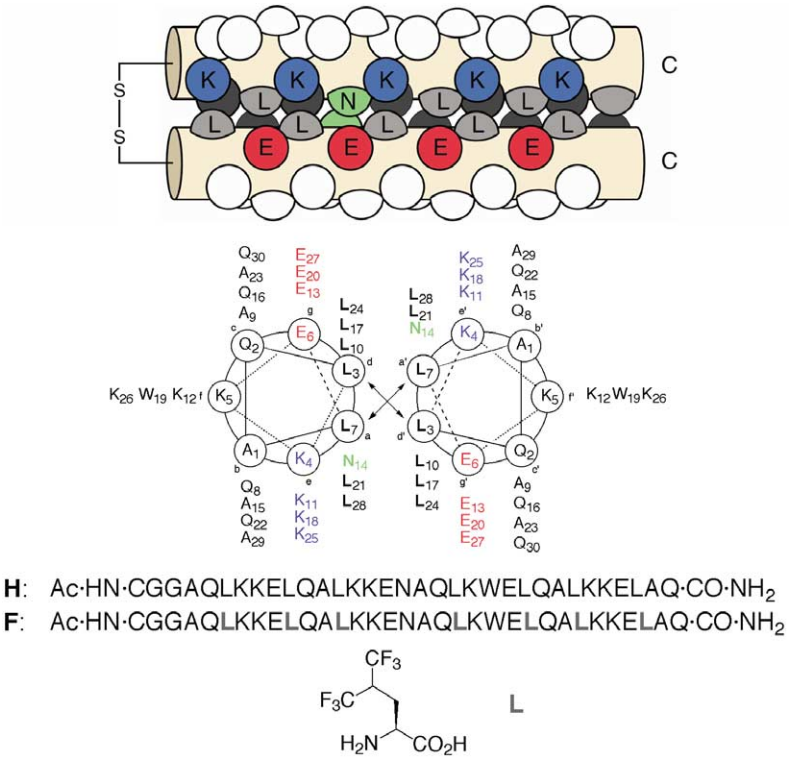

Figure 1. Schematic representation of peptide sequences **HH** and **FF**. The fluorinated peptide **FF** contains seven hexafluoroleucine residues per helix. All the *e* positions are lysine (blue) and the all *g* positions are glutamic acid (red). There is a single asparagine residue (green) in the core to ensure a parallel orientation. The helices are connected at the N-termini with a disulfide bond.

explore specificity in protein–protein interactions.[16,17b] These protein interaction motifs represent small, synthetically tractable targets for testing hypothetical constructs.[17a] The α-helical coiled coil is typically composed of a number of parallel or antiparallel α-helices wrapped around one another with a shallow left-handed superhelical twist.[18] They contain a heptad repeat, whose positions are denoted *a*–*g*, where the *a* and *d* positions are hydrophobic residues that form the interface between helices, and constitute the primary driving force for oligomerization.[19–21] Additionally, interhelical electrostatic interactions between *e* and *g* residues provide a secondary source of stability.[5,22,23] From the crystal structures of 32-residue synthetic coiled coils, it is estimated that nearly 900 $Å^2$ surface area per helix is buried at a dimeric interface and nearly 1640 $Å^2$ per helix in a tetramer.[19,20] The importance of hydrophobic surface area for coiled coil stability has been extensively studied through the use of de novo designed synthetic peptide models.[24,25] These interaction surfaces are therefore ideally suited to study the effect of fluorination on the driving force and specificity.

We designed peptides **H** and **F** to form parallel dimeric coiled coils.[26] These peptides have an identical sequence except that all seven of the core leucine residues in **H** have been replaced by 5,5,5,5′,5′,5′-*S*-hexafluoroleucine in **F** (Fig. 1), shielding 28 trifluoromethyl groups from aqueous solvent in the canonical fluorinated dimer. We introduced basic residues at all the *e* positions and acidic residues at *g* positions. These side chains ensure that the assembly is parallel due to unfavorable interhelical electrostatic interactions in the antiparallel mode.[27] The core is composed entirely of leucine or hexafluoroleucine, to maximize the buried hydrophobic surface area at the interface, with the exception of a single asparagine at position 14. Previous studies have shown that a single psuedosymmetrically disposed asparagine is important in maintaining the dimeric structure of GCN4.[19,28,29] The asparagine residues hydrogen bond with each other in the core and are thermodynamically destabilizing. However, they result in limiting the assembly to a dimeric structure, by destabilizing alternately folded states that require the burial of the polar asparagine side chain in hydrophobic environments. We incorporated Asn 14 in our design in an attempt to restrict the oligomerization state of the peptide assembly and reinforce the stability of the parallel arrangement. In the antiparallel arrangement, the Asn side chains would not be able to hydrogen bond. Furthermore, in order to aid us in the previously reported self-sorting experiment, a Gly–Gly–Cys tripeptide was appended at the NH_2-terminus.[15] The cysteine residue permits redox chemistry in the form of disulfide–thiol equilibrium, and the two glycine residues provide a flexible linker.

2.2. Synthesis

N-tert-butyloxycarbonyl protected 5,5,5,5′,5′,5′-*S*-hexafluoroleucine was prepared according to a recently developed synthetic route in our laboratories.[30] Peptides were synthesized by the in-situ neutralization protocol for *tert*-Boc synthesis on 0.40 mmol NH_2 equiv. g^{-1} methylbenzhydrylamine (MBHA) resin. At the end of linear synthesis, the formyl protecting group on the tryptophan residue was removed by treatment with 1:10 piperidine in

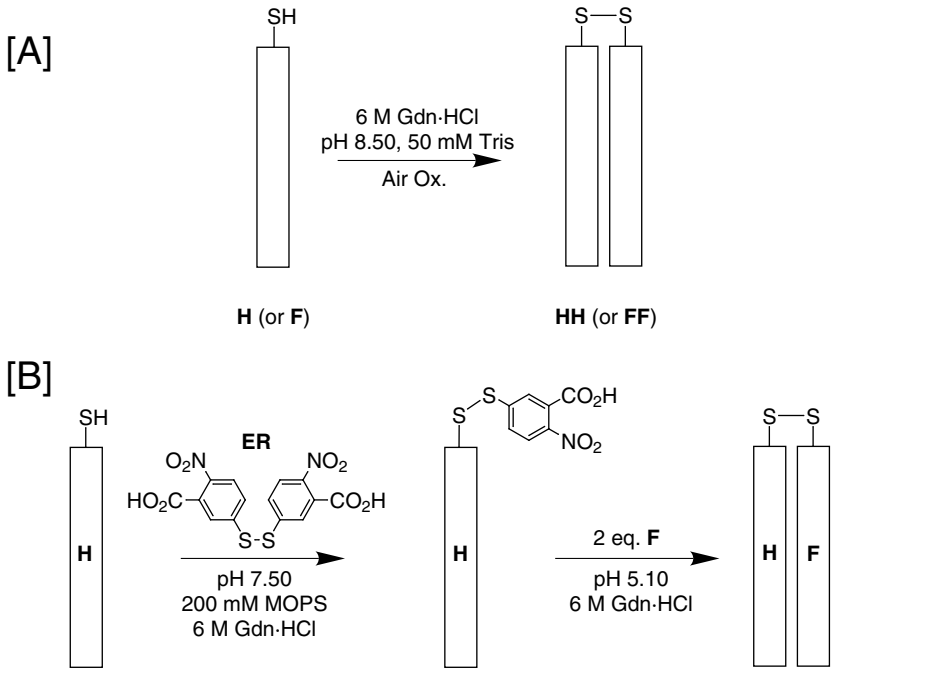

Figure 2. (A) Disulfide bonded homodimers **HH** and **FF** were synthesized by air oxidation of monomeric peptides in 6 M Gdn·HCl. (B) The heterodimer **HF** was synthesized by reaction of **H** with Ellman's reagent (**ER**), followed by reaction with excess **F**.

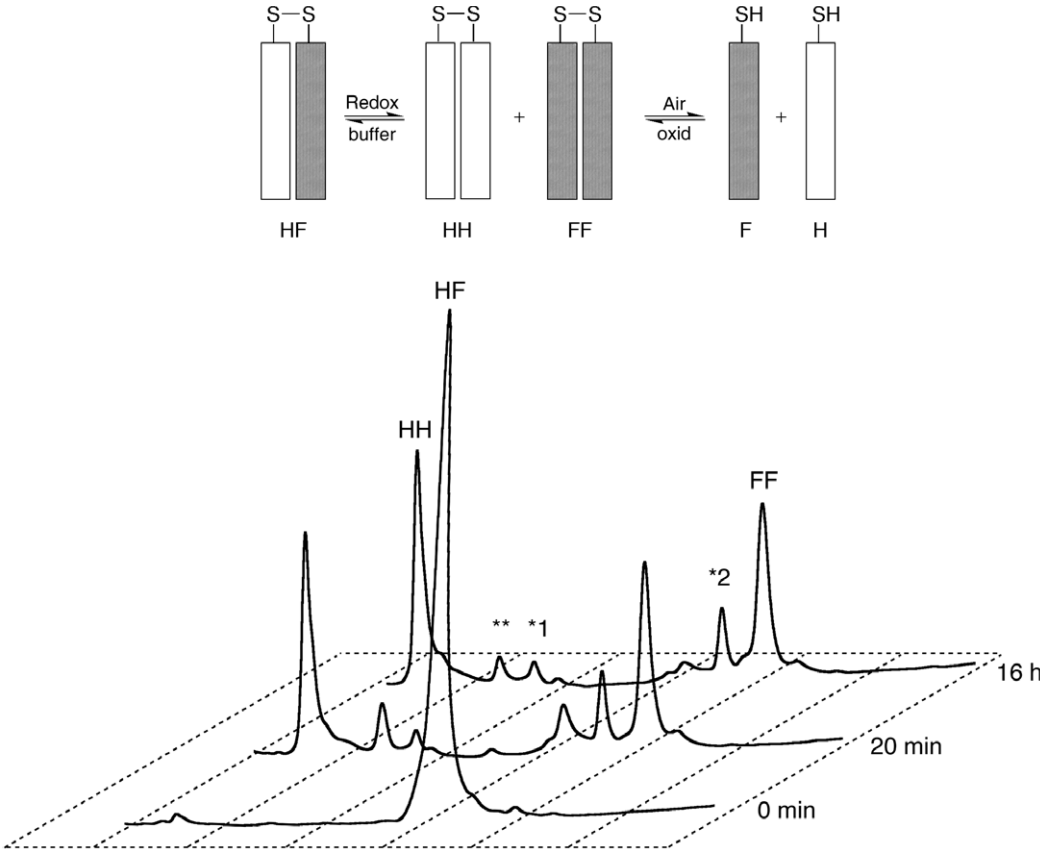

Figure 3. Programmed self-sorting in peptides with hydrocarbon and fluorocarbon cores. HPLC traces showing preferential homodimer formation. Preformed disulfide-bonded heterodimer **HF** (20 μM) was incubated in redox buffer. After ~200 min, equilibrium is established and only homodimers and mixed disulfides remain. The mixed heterodimer is estimated to be less than 2% of all **H** and **F** containing peptides at equilibrium. Peaks marked *1 and *2 are **H** monomer and **F**-glutathione mixed disulfide, respectively, and ** is an impurity. The equilibrium lies firmly in favor of the homodimers **HH** and **FF**. The free energy of specificity for formation of homodimers, $\Delta G_{spec} = -2.1$ kcal/mol.

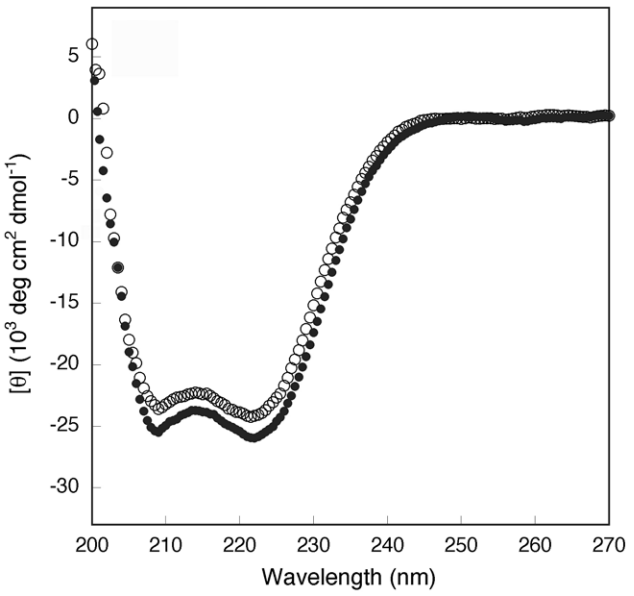

Figure 4. Circular dichroism spectra of **HH** (○) and **FF** (●). Both peptide assemblies are highly helical. Conditions: [**HH**]=[**FF**]=2 μM, pH 7.40, PBS, 10°C.

DMF solution at 0°C for 2 h. Further treatment with anhydrous HF resulted in the simultaneous removal of all side-chain protecting groups and cleavage of the peptide chain from the resin. The peptides were purified on reversed-phase HPLC using a linear gradient of acetonitrile in 0.1% trifluoroacetic acid (TFA)/water. The analytical purity of the peptides was confirmed by HPLC, amino acid analysis and MALDI mass spectrometry.

The disulfide bonded dimers of **H** (**HH**), **F** (**FF**) and the mixed dimer **HF** were synthesized by two different methods. The homodimers **HH** and **FF** were synthesized by overnight air oxidation of the monomeric peptides in 6 M guanidine hydrochloride (Gdn·HCl) at pH 8.50 (50 mM Tris). The heterodimer **HF** was synthesized by reaction of **H** with a large excess of Ellman's reagent (**ER**, CAS No. 69-78-3) to produce an activated disulfide species at pH 7.50, followed by reaction with excess monomeric **F** (Fig. 2) at pH 5.10.[31] The resulting heterodimer **HF** was purified by reversed-phase HPLC.

2.3. Self-sorting and biophysical characterization

We have recently reported that the heterodimeric peptide **HF** self-sorts into the two homodimeric disulfide bonded peptides (Fig. 3).[15] Indeed, when **HF** is incubated in a redox buffer at room temperature, conditions under which disulfide exchange is rapid, the mixed heterodimer cleanly separates into the two homodimers **HH** and **FF**. The reaction was kinetically monitored by removal of aliquots and quenching with 5% acetic acid. The time points were then analyzed by analytical reverse-phase HPLC. Relative amounts of the disulfide-bonded hetero- and homodimers were estimated by integration (Fig. 3). After 200 min, the equilibrium is established, with only a trace of the heterodimer remaining. No further change was observed even after 48 h. From the HPLC data, we find that homodimers are preferred over the heterodimer by at least 26-fold. In

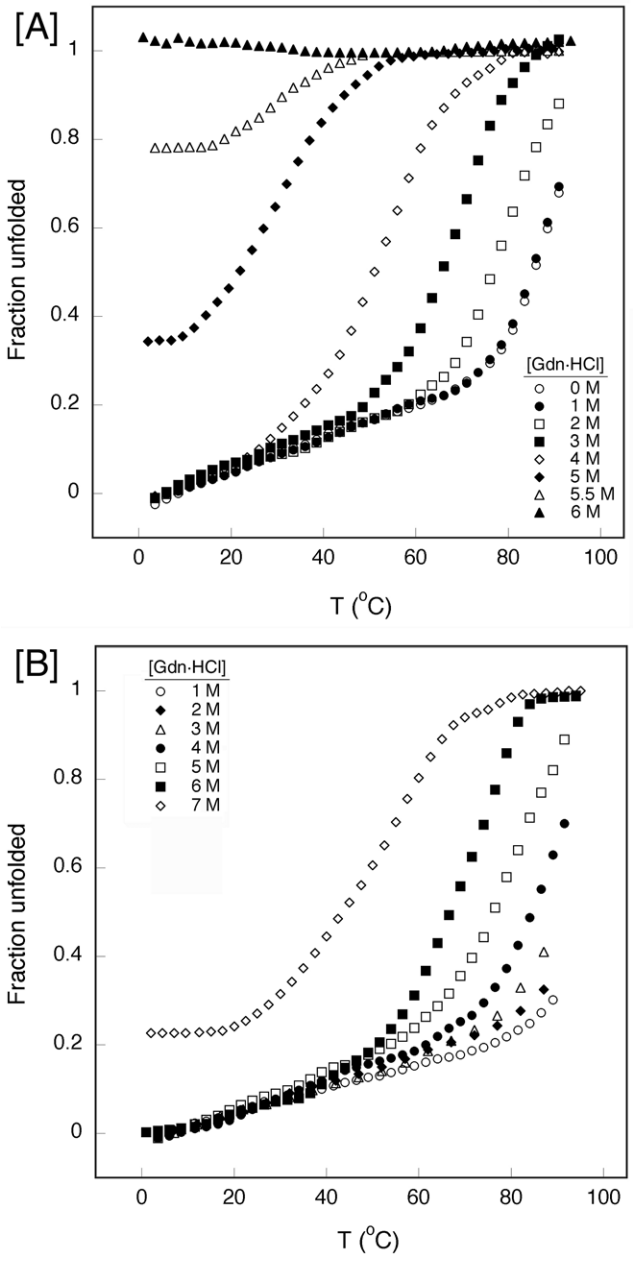

Figure 5. Thermal melting curves for (A) **HH** with increasing concentrations of guanidine hydrochloride and (B) for **FF** monitored by the decrease in molar ellipticity at 222 nm. Peptide concentration=2 μM.

order to confirm that reaction had reached equilibrium, equimolar amounts of the reduced peptides **H** and **F** were placed under similar redox buffer conditions and the reaction was monitored for 16 h. Again, the heterodimer accounted for only 3% of all disulfide-bonded species. Control experiments indicated that the disulfide bond-forming chemistry is reversible and under thermodynamic control, and that there are no kinetic barriers to the formation of the disulfide-bonded heterodimer **HF**. From the peak ratios at equilibrium, the free energy of specificity for the formation of homodimers, ΔG_{spec} is calculated to be at least −2.1 kcal/mol at 20°C.[15] This homodimeric preference of the system is mainly due to hyperstability of the fluorinated peptide assembly (**FF**) and relative instability of the heterodimeric species. We present here a

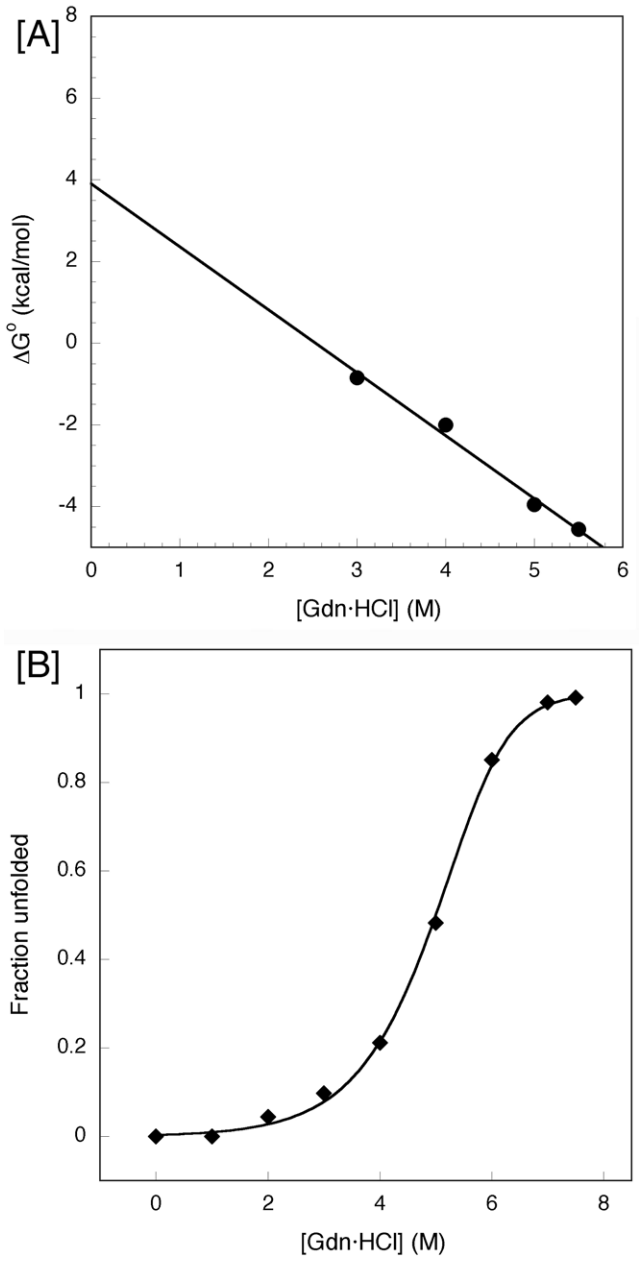

Figure 6. Guanidine·HCl melting curves for (A) **HH** (at 74°C) and (B) **FF** (at 80°C). The data yield an apparent free energy of unfolding: $\Delta G_{\mathbf{HH}}$=+3.90 kcal/mol and $\Delta G_{\mathbf{FF}}$=+16.76 kcal/mol. See text for models and data fitting methods.

detailed thermodynamic comparison of the two homomeric disulfide peptides **HH** and **FF**.

Circular dichroism spectra of **HH** and **FF** peptides reveal a very high degree of α-helicity in both peptides as is expected of a coiled coil structure (Fig. 4). Both peptides exhibit characteristic minima at 208 and 222 nm. Cooperative melting transitions are also observed for both peptides as a function of temperature. Both **HH** and **FF** are extremely stable and do not unfold in benign buffer even at elevated temperatures, but in the presence of chaotropic agents, they show cooperative melting behavior. The fluorinated assembly **FF** is much more stable than **HH** under all conditions tested by us. Indeed, it exhibits a higher melting temperature in buffer and at any concentration of Gdn·HCl. **FF** is an exceptionally robust assembly, resisting even minimal denaturation at room temperature in 6 M Gdn·HCl.

The stabilities of the disulfide bonded dimers were monitored by following the decrease in molar ellipticity at 222 nm in the presence of increasing concentrations of Gdn·HCl (Fig. 5) at various temperatures. The difference in stability is especially striking when one compares the melting temperatures in 5 M Gdn·HCl (ΔT_m=48°C). Relative stabilities can also be obtained by fitting the denaturation data to yield apparent free energies of unfolding. From previously reported sedimentation equilibrium experiments, it is known that **HH** sediments as a monomer (monomeric disulfide bonded species, 2 helices) and **FF** sediments as a dimer (dimer of the disulfide species, 4 helices) in the 2–15 μM concentration range. To accommodate this solution stoichiometry information, two different models were used to extract the free energy of unfolding (Figs. 6 and 7). In the case of **HH**, ΔG° was determined by assuming a two state equilibrium between folded and unfolded states. Data were analyzed by the linear extrapolation method.[32,33] For **FF**, we used an unfolded monomer-folded dimer equilibrium to calculate ΔG° of unfolding (Table 1).[7] The $\Delta\Delta G^{\circ}$ is 13.7 kcal/mol at 74°C,

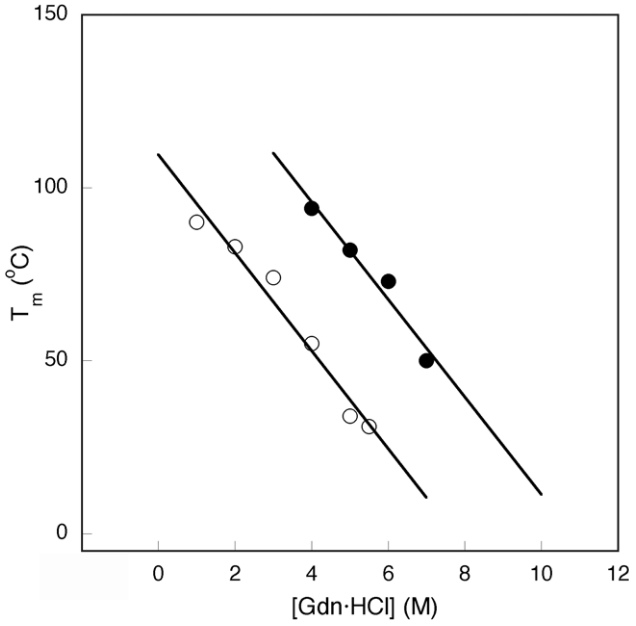

Figure 7. Dependence of melting temperatures (T_m) with Gdn·HCl concentration for **HH** (○) and **FF** (●). At all temperatures, the fluorinated peptide is thermally more stable.

Table 1. Thermodynamic data obtained from temperature and denaturant induced unfolding for peptides **HH**, **FF** and **HF**

Peptide	$\Delta G^{\circ}_{H_2O}$ (kcal/mol)	m (kcal/mol/M)	T_m[a] (°C)	No. of helices[b]
HH	3.90±0.12[c]	1.54±0.06	34	2
HF	–	–	36	2
FF	16.76±0.30[d]	1.51±0.05	82	4

[a] Conditions: 2 μM peptide, pH 7.40, 5 M Gdn·HCl, 10 mM PBS.
[b] By sedimentation equilibrium, data from Ref. 15.
[c] At 74°C assuming a two state folded–unfolded model.
[d] At 80°C assuming a folded dimer–unfolded monomer transition.

clearly establishing the stability order in favor of **FF**. Tirrell and co-workers have also seen enhancement in stability of hexafluoroleucine substituted coiled coil proteins.[34] The thermodynamic consequence of the relative stability of the fluorinated peptide assembly **FF** and the instability of **HF** is to shift the equilibrium away from the heterodimer to the homodimers.

The biophysical studies described here complement our preliminary report of self-sorting coiled coils.[15] The hyperstability of the fluorinated coil alone is sufficient to explain the preference for the homodimers. However, the lower than anticipated stability of the mixed dimer **HF** suggests that the fluorocarbon and hydrocarbon cores are orthogonal and do not like to mix. This study introduces a new paradigm for the design of molecular self-assembling systems, one based on orthogonal solubility properties of liquid phases.

3. Conclusions

Selective fluorination of peptides has recently emerged as a powerful method to alter protein structure. In particular, design utilizing the enhanced hydrophobicity of trifluoromethyl containing side chains has resulted in hyperstable structures. Fluorine can also exert a very powerful inductive effect and this has been utilized to create stable collagen mimics.[35,36] The present study reports the synthesis of protein cores containing hexafluoroleucine and details comparative biophysical studies with peptides containing leucine cores. In general, the fluorinated peptide shows higher thermal stability and enhanced resistance to chemical denaturation. Furthermore, the tendency of mixed hydrocarbon–fluorocarbon cores to self-sort into homomeric bundles suggests new avenues for the design and manipulation of protein–protein interfaces.

4. Experimental

4.1. Peptide synthesis and purification

Peptides were prepared by using the *N-tert*-butyloxycarbonyl (*tert*-Boc) amino acid derivatives for Merrifield manual solid-phase synthesis (MBHA resin), using the in situ neutralization/HBTU protocol typically on a 0.15 mmol scale.[37] *N*-Boc-α-*S*-amino acids were used with the following side chain protecting groups: Asp(OBzl), Asn(Xan), Cys(Acm), Glu(OBzl), Gln(Xan), Lys(2-Cl-Z), and Trp(For). Peptide coupling reactions were carried out with a fourfold excess (0.6 mmol) of activated amino acid for at least 15 min. In the case of hexafluoroleucine, the coupling time was extended to 2 h. The extent of reaction was verified by a Kaiser test after each coupling. The N-terminal was acetylated by treatment with 1:4 acetic anhydride/DMF and 6 equiv. of diisopropylethylamine. The formyl protecting group on the tryptophan residue was removed by treating the resin with 1:10 piperidine in DMF solution. Peptides were cleaved from the resin by using high HF conditions (90% anhydrous HF/10% anisole at 0°C for 1.5 h). Crude peptides were extracted with 25% acetic acid and lyophilized. Freeze dried material was dissolved in 0.1% TFA, desalted and purified by reversed phase HPLC [Vydac C4 column with a 30 min linear gradient of acetonitrile/H_2O/0.1% TFA at 8.0 mL/min].

HH: An aqueous solution of **H** (10 mg, 2.64 μmol) in 50 mM Tris (pH 8.50) and 6 M Gdn·HCl (total volume: 0.75 mL) was stirred overnight at room temperature. The reaction was quenched by addition of 250 μL glacial acetic acid and diluted with 1 mL water. The mixture was directly purified by reversed phase HPLC. The fractions containing **HH** were collected and lyophilized to deliver 9.0 mg (90%) of **HH**. MALDI-MS: MW_{calcd}=7556.8, found: 7561.

FF: An aqueous solution of **F** (14 mg, 3.09 μmol) in 50 mM Tris (pH 8.50) and 6.5 M Gdn·HCl (total volume: 1 mL) was stirred overnight at room temperature. The reaction was quenched by addition of 300 μL glacial acetic acid and diluted with 1.5 mL water. The mixture was directly purified by reversed phase HPLC. The fractions containing **FF** were pooled and lyophilized to deliver 12.1 mg (86%) of **FF**. MALDI-MS: MW_{calcd}=9066, found: 9076.3.

HF: To an aqueous solution of **H** (8 mg, 2.11 μmol) in MOPS buffer (pH 7.50) was added 5,5′-dithiobis(2-nitrobenzoic acid) (20 mg, 50.4 μmol). The reaction was stirred for 15 min and then quenched by the addition of 300 μL of neat TFA. The reaction mixture was then extracted with 4×10 mL Et_2O. The aqueous layer was then directly injected into a reversed-phase C18 column and purified. The fractions containing the mixed disulfide of the Ellman's reagent and **H** were combined and lyophilized to obtain 8.4 mg of the desired product (95%). The mixed disulfide (8 mg, 1.92 μmol) was dissolved in a pH 1.50 solution containing **F** (17.4 mg, 3.84 μmol). The pH was carefully adjusted to 5.10 by sequential addition of 0.1N NaOH solution. The reaction was allowed to proceed for 20 min and then quenched by addition of 300 μL TFA. The reaction mixture was then directly purified by reversed phase HPLC to obtain 10 mg of pure **HF** (62.6%). Nearly 25% of the starting mixed disulfide was recovered unreacted. MALDI-MS: MW_{calcd}: 8310.4, found: 8317.

4.2. Circular dichroism

Circular dichroism studies were performed on a JASCO J-715 spectropolarimeter fitted with a PTC-423S single position Peltier temperature controller using a 1 cm pathlength cuvette (Varian). Buffer conditions were usually 10 mM phosphate (pH 7.40), 137 mM NaCl, 2.7 mM KCl unless otherwise noted. The spectrometer was calibrated with an aqueous solution of recrystallized d_{10}-(+)-camphorsulfonic acid at 290.5 nm. The concentrations of the peptide stock solutions were determined by duplicate amino-acid analysis runs. Mean residue ellipticities (deg cm^2 $dmol^{-1}$) were calculated using the relation:

$$[\theta] = \theta_{obs}\mathrm{MRW}/10{\cdot}l{\cdot}c \quad (1)$$

where θ_{obs} is the measured signal (ellipticity) in millidegrees, l is the optical pathlength of the cell in cm, c is concentration of the peptide in mg/mL and MRW is the mean residue molecular weight (molecular weight of the peptide divided by the number of residues). Thermal denaturation studies were carried out at the concentrations

indicated by monitoring the change in $[\theta]_{222}$ as a function of temperature. Temperature was increased in steps of 0.5°C with an intervening equilibration time of 120 s. Data was collected over 16 s per point. The T_m was determined from the minima of the first derivative of $[\theta]_{222}$ with T^{-1}, where T is in K. All reported T_ms are those obtained from curve fitting.

4.3. Data fitting

The free energy of unfolding for **HH** was determined by assuming a two state equilibrium between folded and unfolded states.

$$F_{\mathbf{HH}} \rightleftharpoons U_{\mathbf{HH}}$$

where $F_{\mathbf{HH}}$ is the folded species and $U_{\mathbf{HH}}$ represents the fully unfolded **HH**. Data were obtained by monitoring $[\theta]_{222}$ as a function of Gdn·HCl concentration. Data were analyzed by the linear extrapolation method to yield the free energy of unfolding. The equilibrium constant and therefore ΔG° are easily determined from the average fraction of unfolding. Assuming that the linear dependence of ΔG° with denaturant concentration in the transition region continues to zero concentration, the data can be extrapolated to obtain $\Delta G^{\circ}_{H_2O}$, the free energy difference in the absence of denaturant.[32,33]

Previously reported sedimentation equilibrium experiments suggest **FF** is a tetramer (dimer of the disulfide bonded dimer) in the 2–15 μM concentration range.[7] Therefore, we used a unfolded monomer-folded dimer equilibrium to calculate ΔG° of unfolding.

$$F_{\mathbf{FF}} \rightleftharpoons 2 \cdot U_{\mathbf{FF}}$$

where $K_d=[U_{\mathbf{FF}}]^2/[F_{\mathbf{FF}}]$ ($U_{\mathbf{FF}}$=unfolded **FF** and $F_{\mathbf{FF}}$=folded dimer of **FF** with 4 helices). Since the total peptide concentration P_t, can be given by $P_t=2[F_{\mathbf{FF}}]+[U_{\mathbf{FF}}]$, the observed CD signal Y_{obs} can be described in terms of folded and unfolded baselines, Y_{fol} and Y_{unfol}, respectively, by the following expression.

$$Y_{obs} = (Y_{unfol} - Y_{fol})\frac{\sqrt{K_d^2 + 8K_dP_t} - K_d}{4P_t} + Y_{fol} \quad (2)$$

Additionally, K_d can be expressed in terms of the free energy of unfolding.

$$K_d = \exp(-\Delta G^{\circ}/RT) \quad (3)$$

Assuming that the apparent free energy difference between folded $F_{\mathbf{FF}}$ and unfolded $U_{\mathbf{FF}}$ states is linearly dependent on the Gdn·HCl concentration, ΔG° can be written as:

$$\Delta G^{\circ} = \Delta G^{\circ}_{H_2O} - m[\text{Gdn·HCl}] \quad (4)$$

where $\Delta G^{\circ}_{H_2O}$ is the free energy difference in the absence of denaturant and m is the dependency of the unfolding transition with respect to the concentration of Gdn·HCl. The data was fit for two parameters, namely $\Delta G^{\circ}_{H_2O}$ and m by nonlinear least squares fitting (KaliedaGraph v3.5).

Acknowledgements

The authors thank Tufts University for support. We thank Dr Xuechao Xing and Alfio Fichera for synthesis of hexafluoroleucine. We also thank Professor David Walt and Professor Marc d'Alarcao for helpful and stimulating discussions.

References

1. Creighton, T. E. *Proteins: Structures and Molecular Properties*; 2nd ed; Freeman: New York, 1993.
2. Tanford, C. *Science* **1978**, *200*, 1012–1018.
3. Kauzmann, W. *Adv. Protein Chem.* **1959**, *14*, 1–63.
4. Yu, Y. H.; Monera, O. D.; Hodges, R. S.; Privalov, P. L. *J. Mol. Biol.* **1996**, *255*, 367–372.
5. Lumb, K. J.; Kim, P. S. *Science* **1995**, *268*, 436–439.
6. Aurora, R.; Rose, G. D. *Protein Sci.* **1998**, *7*, 21–38.
7. Bilgiçer, B.; Fichera, A.; Kumar, K. *J. Am. Chem. Soc.* **2001**, *123*, 4393–4399.
8. Tang, Y.; Ghirlanda, G.; Vaidehi, N.; Kua, J.; Mainz, D. T.; Goddard, W. A.; DeGrado, W. F.; Tirrell, D. A. *Biochemistry* **2001**, *40*, 2790–2796.
9. Israelachvili, J. N.; Mitchell, D. J.; Ninham, B. W. *Biochim. Biophys. Acta* **1977**, *470*, 185–201.
10. Tanford, C. *The Hydrophobic Effect: Formation of Micelles and Biological Membranes*; 2nd ed; Wiley: New York, 1980.
11. Resnati, G. *Tetrahedron* **1993**, *49*, 9385–9445.
12. Riess, J. G. *Coll. Surf., A* **1994**, *84*, 33–48.
13. Scott, R. L. *J. Am. Chem. Soc.* **1948**, *70*, 4090–4093.
14. Marsh, E. N. G. *Chem. Biol.* **2000**, *7*, R153–R157.
15. Bilgiçer, B.; Xing, X.; Kumar, K. *J. Am. Chem. Soc.* **2001**, *123*, 11815–11816.
16. Lupas, A. *Curr. Opin. Struct. Biol.* **1997**, *7*, 388–393.
17. (a) Lajmi, A. R.; Lovrencic, M. E.; Wallace, T. R.; Thomlinson, R. R.; Shin, J. A. *J. Am. Chem. Soc.* **2000**, *122*, 5638–5639. (b) Lupas, A. *Trends Biochem. Sci.* **1996**, *21*, 375–382.
18. Crick, F. H. C. *Acta Crystallogr.* **1953**, *6*, 689–697.
19. Harbury, P. B.; Zhang, T.; Kim, P. S.; Alber, T. *Science* **1993**, *262*, 1401–1407.
20. O'Shea, E. K.; Klemm, J. D.; Kim, P. S.; Alber, T. *Science* **1991**, *254*, 539–544.
21. O'Shea, E. K.; Rutkowski, R.; Kim, P. S. *Science* **1989**, *243*, 538–542.
22. Monera, O. D.; Zhou, N. E.; Kay, C. M.; Hodges, R. S. *J. Biol. Chem.* **1993**, *268*, 19218–19227.
23. Monera, O. D.; Kay, C. M.; Hodges, R. S. *Biochemistry* **1994**, *33*, 3862–3871.
24. Zhu, B. Y.; Zhou, N. E.; Kay, C. M.; Hodges, R. S. *Protein Sci.* **1993**, *2*, 383–394.
25. Zhu, B. Y.; Zhou, N. E.; Semchuk, P. D.; Kay, C. M.; Hodges, R. S. *Int. J. Pept. Protein Res.* **1992**, *40*, 171–179.
26. The program MultiCoil predicted a 98% probability for a dimeric state for **HH**.Wolf, E.; Kim, P. S.; Berger, B. *Protein Sci.* **1997**, *6*, 1179–1189.
27. Oshea, E. K.; Lumb, K. J.; Kim, P. S. *Curr. Biol.* **1993**, *3*, 658–667.
28. Akey, D. L.; Malashkevich, V. N.; Kim, P. S. *Biochemistry* **2001**, *40*, 6352–6360.
29. Lumb, K. J.; Kim, P. S. *Biochemistry* **1995**, *34*, 8642–8648.

30. Xing, X.; Fichera, A.; Kumar, K. *Org. Lett.* **2001**, *3*, 1285–1286.
31. Riddles, P. W.; Blakeley, R. L.; Zerner, B. *Meth. Enzymol.* **1983**, *91*, 49–60.
32. Pace, C. N. *Meth. Enzymol.* **1995**, *259*, 538–554.
33. Tanford, C. *Adv. Protein Chem.* **1962**, *17*, 69–165.
34. Tang, Y.; Tirrell, D. A. *J. Am. Chem. Soc.* **2001**, *123*, 11089–11090.
35. Bretscher, L. E.; Jenkins, C. L.; Taylor, K. M.; DeRider, M. L.; Raines, R. T. *J. Am. Chem. Soc.* **2001**, *123*, 777–778.
36. Holmgren, S. K.; Bretscher, L. E.; Taylor, K. M.; Raines, R. T. *Chem. Biol.* **1999**, *6*, 63–70.
37. Schnölzer, M.; Alewood, P.; Jones, A.; Alewood, D.; Kent, S. B. H. *Int. J. Pept. Protein Res.* **1992**, *40*, 180–193.